

# Preparation, Characterization, and Antibacterial Activity of Green-Biosynthesised Silver Nanoparticles using *Clinacanthus nutans* Extract

Salahaedin Waiezi<sup>1</sup>, Nik Ahmad Nizam Nik Malek<sup>1,2,\*</sup> , Muhammad Hariz Asraf<sup>1</sup> ,  
Nor Suriani Sani<sup>3</sup> 

<sup>1</sup> Department of Biosciences, Faculty of Science, Universiti Teknologi Malaysia, 81310 UTM, Skudai, Johor, Malaysia; salahaedinw@gmail.com (S.W.);

<sup>2</sup> Centre for Sustainable Nanomaterials (CSNano), Ibnu Sina Institute for Scientific and Industrial Research (ISI-ISIR), Universiti Teknologi Malaysia, 81310 UTM Johor, Malaysia; nikhizam@utm.my (N.A.N.N.M);

<sup>3</sup> Office of Deputy Vice-Chancellor (Research and Innovation), Universiti Teknologi Malaysia, 81310 UTM, Skudai, Johor, Malaysia; norsuriani@utm.my (N.S.S.);

\* Correspondence: nikhizam@utm.my (N.A.N.N.M.);

Scopus Author ID 35995651900

Received: 5.02.2022; Accepted: 7.03.2022; Published: 30.03.2022

**Abstract:** Plant leaf extract can be used as a reducing agent in the synthesis of silver nanoparticles (AgNP) in a green and safe way. As a result, this study describes the synthesis of AgNP using a *Clinacanthus nutans* plant extract. *C. nutans* is known as belalai gajah in Malaysia and is widely used as a medicinal herb. UV-Vis spectroscopy, X-ray diffraction (XRD), field emission scanning electron microscopy (FESEM), energy dispersive X-ray (EDX), and transmission electron microscope (TEM) were used to characterize the biosynthesized AgNP using *C. nutans* aqueous extract at pH 10, 70°C, and a reaction time of 48 hours. The UV-Vis spectra revealed a peak around 400 nm, while XRD confirmed AgNP's crystal structure, which had an average size of 20 to 30 nm, as shown in FESEM and TEM micrographs. The antibacterial activity of biosynthesized AgNP against *Escherichia coli*, *Pseudomonas aeruginosa*, and *Staphylococcus aureus* was tested using the disc diffusion technique (DDT). Antibacterial activity was limited against *Enterococcus faecalis* and methicillin-resistant *Staphylococcus aureus* (MRSA). AgNP, which was synthesized using *C. nutans* leaf extract AgNP as a bioreducing agent, has antibacterial activity against a wide range of bacteria in general.

**Keywords:** silver nanoparticles; *Clinacanthus nutans*; antibacterial agent; biosynthesis.

© 2022 by the authors. This article is an open-access article distributed under the terms and conditions of the Creative Commons Attribution (CC BY) license (<https://creativecommons.org/licenses/by/4.0/>).

## 1. Introduction

Metal nanoparticles could be synthesized via several techniques, such as radiation, chemical precipitation, photochemical, and electrochemical techniques. However, the methods pose several disadvantages, such as being costly, toxic, producing heterogeneous particle size, flammable, damaging the environment, or producing biological risk [1-6]. Thereby, researchers are compelled to identify and find alternative and reliable methods to synthesize the nanoparticles due to the rapid development of nanoparticles, especially silver nanoparticles (AgNP), together with their wide applications and growing global demand. Green synthesis is a reliable method to synthesize AgNP, involving bioresources as the reducing agent in the reduction process of  $\text{Ag}^+$  to  $\text{Ag}^0$  (AgNP), compared to conventional synthesis methods [7-12]. The utilization of plant extract (bioresource material) is a preferred approach for AgNP

synthesis, and it is a good example of green synthesis. It is relatively cheap environmentally friendly, and it can be easily found due to its abundance in nature [10,11]. The key factor in using plant extract in AgNP synthesis is that the plant biomolecules and secondary metabolites help reduce and stabilize the Ag ions during the biosynthesis process [11-15].

The use of AgNP is increasing due to its ability to prevent and kill pathogenic microorganisms besides its wide usage in various products such as food packaging, plastics, soaps, pastes, food, and especially in hospitals for different medical equipment types [11,14]. The biological technique of AgNP synthesis lacks the utilization and production of toxic materials and expensive chemicals because it employs natural reducing, capping, and stabilizing agents. Plant extracts contain various combinations of biomolecules with proven medicinal values, i.e., carbohydrates, amino acids, enzymes, proteins, alcohols, aromatic phenols compounds, and polyphenols [12,15]. Additionally, the production of AgNP from plants renders various benefits such as rapid reaction, non-pathogenic, biocompatibility, cheap, single-step synthesis, easily available, safe to handle, and minimal toxicity to the environment.

Hence, this paper reports the synthesis of AgNP from a Malaysian local herb named *Clinacanthus nutans* (a family of *Acanthaceae*) or locally known as *belalai gajah*. The extracted leaves of *C. nutans* are known for their significant healthcare role, and they are widely used in cancer treatment due to their cost-effectiveness [13,14]. The phytochemical analysis of this plant exhibits a wide range of bioactive components such as flavonoids, glycosides, glycolipids, cerebrosides, and monoacyl monogalactosyl glycerol [13-16]. The study further explained that the pharmacological analysis of *C. nutans* had discovered the antimicrobial activity, anti-inflammatory, antiviral, antioxidant, and anti-diabetic actions. It has been used in different applications such as skin rashes, snake and insect bites, diabetes, and gout management. This work highlighted the potential of *C. nutans* in synthesizing AgNP as an environmentally-friendly, cheap, and easy synthesis method and readily available raw material.

## 2. Materials and Methods

### 2.1. Preparation of plant extract.

The leaves of *C. nutans* were collected from Nursery Rimbun Ventures, Johor, Malaysia. The fresh and healthy leaves were washed with deionized water and left to dry at room temperature for a week. The dried leaves were crushed and ground into a powder form and stored at 4°C for future use. About 2.0 g of the powder was added to 100 mL deionized water (2 %, w/v) and subsequently heated at 100°C using a hotplate magnetic stirrer for 15 min. Then, the plant extract was filtered and kept at 4°C for further assessment.

### 2.2. Biosynthesis of silver nanoparticles.

For the biosynthesis of AgNP, 1.0 mL of leaf extract was added to 10 mL of AgNO<sub>3</sub> 1.0 mM (VChem Laboratory Chemicals). Our preliminary experiment showed that the optimum parameters (data not shown) for synthesizing AgNP using *C. nutans* aqueous extract were at pH 10, the reaction temperature of 70°C, and 48 h reaction time. The UV-Visible spectroscopic analysis was performed using the 7205 UV/Vis spectrophotometer (Jenway, UK) at the wavelength of 360 nm to 750 nm to monitor the production of AgNP.

The colloidal form of AgNP was centrifuged at 10,000 rpm at 40°C for 15 min. The supernatant was discarded, and deionized water was added to the pellet several times until a clear solution was obtained. Finally, the powder was dried in an oven at 50°C for 24 h.

### 2.3. Characterisation.

The characterization of the biosynthesized AgNPs was performed using the X-ray diffraction (XRD, Rigaku SmartLab, Japan) equipment. The XRD pattern was recorded with CuK $\alpha$  radiation at 40 kV with the range of  $2\theta$  at 20–100°. A transmission electron microscope (TEM, model JEOL JEM-ARM 200F, Japan) operated at 200 kV was used for AgNP morphological analysis. The sample powder was initially dissolved in 3 mL ethanol and sonicated for 30 min in the TEM analysis. The sample was then dropped onto a carbon copper grid (about 2–3 drops) and dried in a vacuum pump before viewing under the TEM. A field emission scanning electron microscope (FESEM, model Hitachi SU8020, Japan) was used for AgNP surface morphology analysis. The AgNP powder was observed at different magnifications. The FESEM instrument is equipped with a dispersive energy X-ray (EDX) analyzer for elemental analysis. The scanning of the sample for EDX analysis was obtained from 0 to 20 keV at several sites.

### 2.4. Antibacterial assay.

The antibacterial activity of the sample was assessed against Gram-negative (*Escherichia coli* ATCC 11229 and *Pseudomonas aeruginosa* ATCC 15442) and Gram-positive bacteria (*Staphylococcus aureus* ATCC 6538 and methicillin-resistant *Staphylococcus aureus* [MRSA] ATCC 43300) based on the disk diffusion technique (DDT) [14, 17]. A total of three bacterial colonies were inoculated into a saline solution (0.9%), and the turbidity was monitored and matched to the 0.5 McFarland standard that contained approximately  $1.5 \times 10^8$  colony-forming unit (CFU)/mL (Clinical and Laboratory Standards Institute, 2014). The bacteria were then spread evenly onto the Muller-Hinton agar plate. The discs containing colloidal biosynthesized AgNP (100 and 200  $\mu$ L) and plant aqueous extract (control) were placed on the agar, and the plates were incubated in an incubator (37°C) overnight. The inhibition zone around the disc was measured using a ruler (in mm).

## 3. Results and Discussion

### 3.1. Characterisation of biosynthesized silver nanoparticles.

The production of colloidal biosynthesized AgNP was monitored using UV-Vis spectroscopic technique. Figure 1 (a) shows the UV-Vis spectra of AgNP colloidal formation at different pH values (pH 9, 10, and 11) during the AgNP reaction. The peak appeared in the range of 390 to 430 nm, representing the production of synthesized AgNPs. The production, stability, and morphology of the biosynthesized AgNP were influenced by pH value. At lower pH, the active components of *C. nutans* are ineffective in reducing Ag ions due to their structural stability through H-bonding.

On the contrary, the NO $_3^-$  group of AgNO $_3$  is a stronger oxidant than Ag. At basic pH (higher pH), the Ag ions formed Ag $_2$ O, reducing to AgNPs [18-20]. The phytochemical components in *C. nutans* are responsible for reducing, stabilizing, and capping agents for the biosynthesized AgNP.

The powdered biosynthesized AgNP was characterized for its structure using XRD (Figure 1 [b]). Several peaks are observed in the XRD pattern, at  $2\theta$ , i.e.,  $28^\circ$ ,  $32^\circ$ ,  $45^\circ$ ,  $55^\circ$ ,  $57^\circ$ ,  $75^\circ$ ,  $78^\circ$ , and  $85^\circ$ , attributed to the planes of 111, 200, 220, 311, 222, 400, 420, and 422 reflections on the face-centered of crystalline AgNP cubic structure. Other peaks are observed, which may contribute to the crystalline impurities of the plant extract.

The morphology and elemental analyses of the biosynthesized AgNP are shown in Fig. 2 for FESEM image (Figure 2[a]), elemental analysis using EDX (Figure 2[b]), and TEM images at two different magnifications (Figure 2[c–d]). The AgNP is observed with sizes ranging between 20 to 30 nm. The TEM results displayed various shapes of the biosynthesized AgNP particles, i.e., spherical, quasi-spherical, hexagonal, ellipsoidal, and irregular with diverse diameter sizes. Furthermore, the edge of the biosynthesized AgNP is lighter than the center, proving that the biomolecules from the *C. nutans* are responsible for AgNP capping [21-24]. Meanwhile, the EDX result shows the peaks for carbon (C), oxygen (O), chlorine (Cl), sulfur (S), and phosphorus (P) that may originate from the biomolecules of *C. nutans*, attached to the AgNP and the organic compounds present in the *C. nutans* extract. The EDX spectrum shows a significant peak of elemental Ag, representing the formation of AgNP. On the contrary, the other peaks related to the C, Cl, O, S, and P are active molecules of *C. nutans* responsible for reducing  $\text{Ag}^+$  to  $\text{Ag}^0$ .

UV-Vis spectra demonstrated the production of AgNP due to the emergence of the surface plasmon resonance (SPR) at around 400 nm. Additionally, the crystal structure of AgNPs was confirmed by the XRD pattern. Meanwhile, the morphological analysis from FESEM and TEM specified that the average size of AgNP is between 20 to 30 nm. Hence, the characterization analysis proves the potential of *C. nutans* as the reducing agent of  $\text{Ag}^+$  to AgNP and further as a capping agent through its phytochemical compounds.

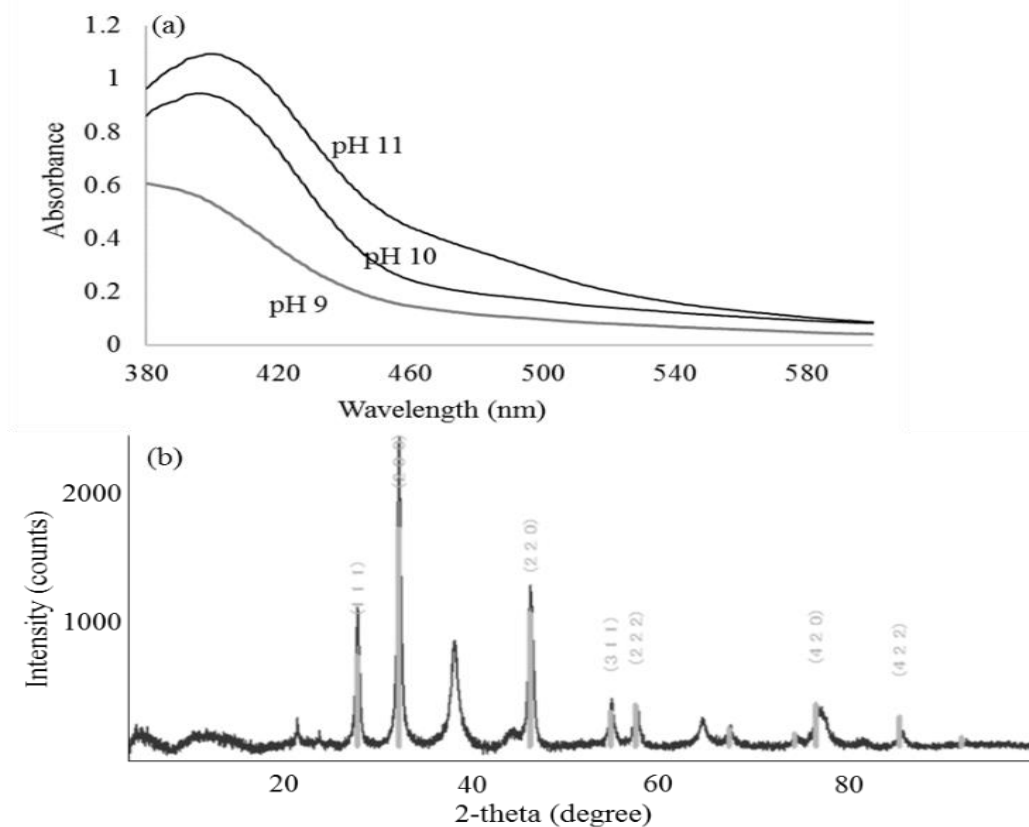


**Figure 1.** (a) UV-Vis spectra of biosynthesized AgNP at different pH; (b) X-ray diffractogram of the biosynthesized at pH 10.

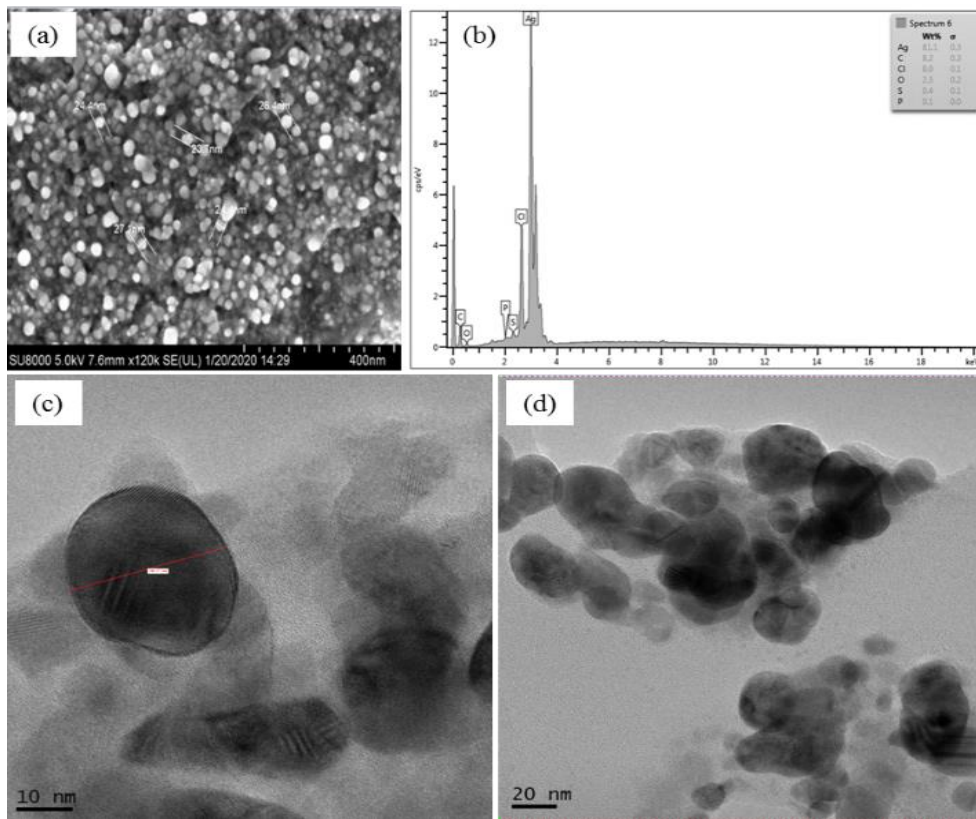


**Figure 2.** (a) FESEM image; (b) EDX spectrum; and (c and d) TEM images of the biosynthesized AgNP.

### 3.2. Antibacterial activity of biosynthesized silver nanoparticles.

DDT is an antibacterial sensitivity test against synthesized materials. In this research, the antibacterial activity of the biosynthesized AgNP using *C. nutans* was tested against Gram-negative (*E. coli* ATCC 11229 and *P. aeruginosa* ATCC 15442) and Gram-positive (*S. aureus* ATCC 6538 and MRSA ATCC 43300) bacteria. Figure 3 depicts the images of the studied bacteria using synthesized AgNP from *C. nutans* extract, while Table 1 shows the values of the inhibition zones.

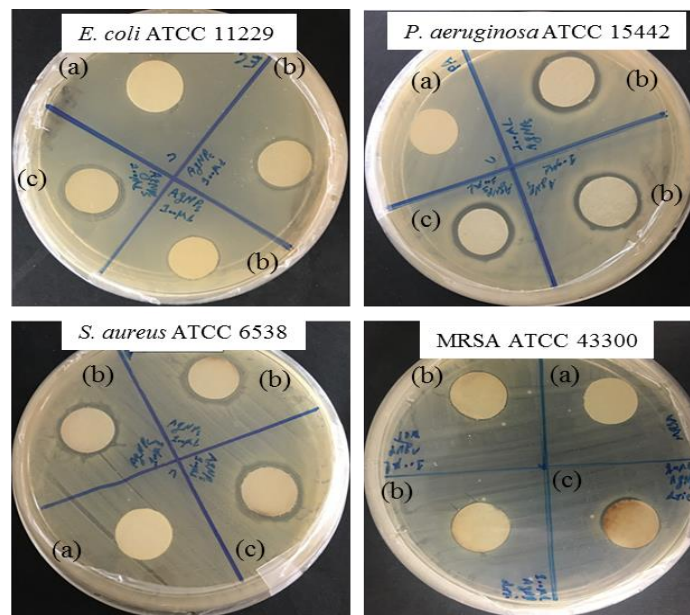


**Figure 3.** DDT images of the biosynthesized AgNP against different types of bacteria and different volumes (a) control; (b) 100 µL; (c) 200 µL.

**Table 1.** Zone of inhibition values of the biosynthesized AgNP against different types of bacteria.

Bacteria	Zone of Inhibition (mm) of synthesized AgNP using <i>C. nutans</i>		
	Control	100 $\mu$ L	200 $\mu$ L
<i>E. coli</i> ATCC11229	0	18	21
<i>P. aeruginosa</i> ATCC15442	0	18	22
<i>S. aureus</i> ATCC6538	0	18.5	21
MRSA ATCC4330	0	17	18

In this research, the biosynthesized AgNP showed a remarkable inhibition zone on all tested bacteria (Table 1). AgNP revealed a better antibacterial efficacy against *P. aeruginosa*, *E. coli*, and *S. aureus* with larger inhibition zones than the mild inhibitory effect against MRSA (Figure 3). These results indicate that the antibacterial activity of AgNP could be associated with the characteristics of certain bacterial species. The smaller zone of inhibition exerted by AgNP against MRSA might be derived from the differences in its membrane structure.

A study reported that the antibacterial mechanism of AgNP was due to the inhibitory effect of the Ag ions in the form of electrostatic attraction, which could penetrate and disrupt the bacterial cell wall. This occurs when the positively charged Ag ions are attached to the negatively charged cell membrane [25-27]. Based on a report, the differences in the cell wall such as structure, thickness, and composition could be the reason for Gram-negative bacteria being more sensitive and showing a substantial inhibition to the AgNP than Gram-positive bacteria, even at a low concentration [28-30].

Furthermore, the susceptibility of Gram-negative bacteria could be due to the layer of lipopolysaccharides and peptidoglycans comprised in the cell wall [31-33]. The arrangement of the cell wall of Gram-negative bacteria facilitates the entry of free ions from the nanoparticles into the cell. *E. coli* is more negatively charged and rigid than *S. aureus* [34-36]. In contrast, the lack of inhibition zone in MRSA may be related to the structure of cell wall and high concentration of bacteria due to multiple colonies, leading to the lack of expression of the antibacterial activity.

#### 4. Conclusions

The AgNP was successfully synthesized using an aqueous extract of *C. nutans* leaves at 70°C, pH 10, and 48 h reaction time. The biosynthesized AgNP has an average of 20–30 nm and is effective against the tested Gram-positive and Gram-negative bacteria, except MRSA. Hence, the potential of *C. nutans* to replace the chemical synthesis method is established with an extended antibacterial activity application.

#### Funding

This research received funding from Fundamental Research Grant Scheme (FRGS) (Vot No: 5F291) and UTM Transdisciplinary Research Grant (TDR; Vot No: 06G71 and 06G72).

#### Acknowledgments

The authors would like to thank Universiti Teknologi Malaysia and the Ministry of Higher Education Malaysia for the financial support under the Fundamental Research Grant Scheme (FRGS) (Vot No: 5F291) and UTM Transdisciplinary Research Grant (TDR; Vot No: 06G71 and 06G72).

## Conflicts of Interest

The authors declare that they have no competing interests.

## References

1. Narayanan, M.; Divya, S.; Natarajan, D.; Senthil-Nathan, S.; Kandasamy, S.; Chinnathambi, A.; Alahmadi, T.A.; Pugazhendhi, A. Green synthesis of silver nanoparticles from aqueous extract of *Ctenolepis garcini* L. and assess their possible biological applications. *Process Biochem.* **2021**, *107*, 91-99, <https://doi.org/10.1016/j.procbio.2021.05.008>.
2. Salayová, A.; Bedlovičová, Z.; Daneu, N.; Baláž, M.; Lukáčová Bujňáková, Z.; Balážová, E.; Tkáčiková, E. Green synthesis of silver nanoparticles with antibacterial activity using various medicinal plant extracts: Morphology and antibacterial efficacy. *Nanomaterials* **2021**, *11*, 1005, <https://doi.org/10.3390/nano11041005>.
3. Rajkumar, R.; Ezhumalai, G.; Gnanadesigan, M.. A green approach for the synthesis of silver nanoparticles by *Chlorella vulgaris* and its application in photocatalytic dye degradation activity. *Environ. Technol. Innov.* **2021**, *21*, 101282, <https://doi.org/10.1016/j.eti.2020.101282>.
4. Devanesan, S.; AlSalhi, M. S. Green synthesis of silver nanoparticles using the flower extract of *Abelmoschus esculentus* for cytotoxicity and antimicrobial studies. *Int. J. Nanomedicine* **2021**, *16*, 3343, <https://doi.org/10.2147/IJN.S307676>.
5. Veeraraghavan, V.P.; Periadurai, N.D.; Karunakaran, T.; Hussain, S.; Surapaneni, K.M.; Jiao, X. Green synthesis of silver nanoparticles from aqueous extract of *Scutellaria barbata* and coating on the cotton fabric for antimicrobial applications and wound healing activity in fibroblast cells (L929). *Saudi J. Biol. Sci.* **2021**, *28*, 3633-3640, <https://doi.org/10.1016/j.sjbs.2021.05.007>.
6. Mane, P.C.; Sayyed, S.A.; Kadam, D.D.; D Shinde, M.; Fatehmulla, A.; Aldhafiri, A.M.; Alghamdi, E.A.; Amalnerkar, D.P.; Chaudhari, R.D. Terrestrial snail-mucus mediated green synthesis of silver nanoparticles and in vitro investigations on their antimicrobial and anticancer activities. *Sci. Rep.* **2021**, *11*, 1-16, <https://doi.org/10.1038/s41598-021-92478-4>.
7. Alahmad, A.; Feldhoff, A.; Bigall, N.C.; Rusch, P.; Scheper, T.; Walter, J.G. *Hypericum perforatum* L.-mediated green synthesis of silver nanoparticles exhibiting antioxidant and anticancer activities. *Nanomaterials* **2021**, *11*, 487, <https://doi.org/10.3390/nano11020487>.
8. Rodríguez-Félix, F.; López-Cota, A.G.; Moreno-Vásquez, M.J.; Graciano-Verdugo, A.Z.; Quintero-Reyes, I.E.; Del-Toro-Sánchez, C.L.; Tapia-Hernández, J.A. Sustainable-green synthesis of silver nanoparticles using safflower (*Carthamus tinctorius* L.) waste extract and its antibacterial activity. *Heliyon* **2021**, *7*, e06923, <https://doi.org/10.1016/j.heliyon.2021.e06923>.
9. Morales-Lozoya, V.; Espinoza-Gómez, H.; Flores-López, L.Z.; Sotelo-Barrera, E.L.; Núñez-Rivera, A.; Cadena-Nava, R.D.; Alonso-Núñez, G.; Rivero, I.A. Study of the effect of the different parts of *Morinda citrifolia* L.(noni) on the green synthesis of silver nanoparticles and their antibacterial activity. *Appl. Surf. Sci.* **2021**, *537*, 147855, <https://doi.org/10.1016/j.apsusc.2020.147855>.
10. Naghizadeh, A.; Mizwari, Z. M.; Ghoreishi, S. M.; Lashgari, S.; Mortazavi-Derazkola, S.; Rezaie, B. Biogenic and eco-benign synthesis of silver nanoparticles using jujube core extract and its performance in catalytic and pharmaceutical applications: Removal of industrial contaminants and in-vitro antibacterial and anticancer activities. *Environ. Technol. Innov.* **2021**, *23*, 101560, <https://doi.org/10.1016/j.eti.2021.101560>.
11. Khodadadi, S.; Mahdinezhad, N.; Fazeli-Nasab, B.; Heidari, M.J.; Fakheri, B.; Miri, A. Investigating the possibility of green synthesis of silver nanoparticles using *Vaccinium arctostaphylos* extract and evaluating its antibacterial properties. *Biomed Res. Int.* **2021**, *2021*, <https://doi.org/10.1155/2021/5572252>.
12. Wei, S.; Wang, Y.; Tang, Z.; Xu, H.; Wang, Z.; Yang, T.; Zou, T. A novel green synthesis of silver nanoparticles by the residues of Chinese herbal medicine and their biological activities. *RSC Adv.* **2021**, *11*, 1411-1419, <https://doi.org/10.1039/D0RA08287B>.
13. Aryan; Ruby; Mehata, M.S. Green synthesis of silver nanoparticles using *Kalanchoe pinnata* leaves (life plant) and their antibacterial and photocatalytic activities. *Chem. Phys. Lett.* **2021**, *778*, 138760, <https://doi.org/10.1016/j.cplett.2021.138760>.
14. Donga, S.; Chanda, S. Facile green synthesis of silver nanoparticles using *Mangifera indica* seed aqueous extract and its antimicrobial, antioxidant and cytotoxic potential (3-in-1 system). *Artif. Cells Nanomed. Biotechnol.* **2021**, *49*, 292-302, <https://doi.org/10.1080/21691401.2021.1899193>.

15. Al-Sharqi, A.; Apun, K.; Vincent, M.; Kanakaraju, D.; Bilung, L.M.; Sum, M.S.H. Investigation of the antibacterial activity of Ag-NPs conjugated with a specific antibody against *Staphylococcus aureus* after photoactivation. *J. Appl. Microbiol.* **2020**, *128*, 102-115, <https://doi.org/10.1111/jam.14471>.
16. AlSalhi, M.S.; Elangovan, K.; Ranjitsingh, A.J.A.; Murali, P.; Devanesan, S. Synthesis of silver nanoparticles using plant derived 4-N-methyl benzoic acid and evaluation of antimicrobial, antioxidant and antitumor activity. *Saudi J. Biol. Sci.* **2019**, *26*, 970-978, <https://doi.org/10.1016/j.sjbs.2019.04.001>.
17. Isah, M.; Asraf, M.H.; Malek, N.A.N.N.; Jemon, K.; Sani, N.S.; Muhammad, M.S.; Wahab, M.F.A.; Saidin, M.A.R. Preparation and characterization of chlorhexidine modified zinc-kaolinite and its antibacterial activity against bacteria isolated from water vending machine. *J. Environ. Chem. Eng.* **2020**, *8*, 103545, <https://doi.org/10.1016/j.jece.2019.103545>.
18. Bharadwaj, K.K.; Rabha, B.; Pati, S.; Choudhury, B.K.; Sarkar, T.; Gogoi, S.K.; Kakati, N.; Baishya, D.; Kari, Z.A.; Edinur, H.A. Green synthesis of silver nanoparticles using *Diospyros malabarica* fruit extract and assessments of their antimicrobial, anticancer and catalytic reduction of 4-nitrophenol (4-NP). *Nanomaterials* **2021**, *11*, 1999, <https://doi.org/10.3390/nano11081999>.
19. Palithya, S.; Gaddam, S.A.; Kotakadi, V.S.; Penchalaneni, J.; Golla, N.; Krishna, S.B.N.; Naidu, C.V. Green synthesis of silver nanoparticles using flower extracts of *Aerva lanata* and their biomedical applications. *Part. Sci. Technol.* **2021**, 1-13, <https://doi.org/10.1080/02726351.2021.1919259>.
20. Widadalla, H.A.; Yassin, L.F.; Alrasheid, A.A.; Ahmed, S.A.R.; Widdatallah, M.O.; Eltilib, S.H.; Mohamed, A.A. Green synthesis of silver nanoparticles using green tea leaf extract, characterization and evaluation of antimicrobial activity. *Nanoscale Advances* **2022**, *4*, 911-915 <https://doi.org/10.1039/D1NA00509J>.
21. Vanlalveni, C.; Lallianrawna, S.; Biswas, A.; Selvaraj, M.; Changmai, B.; Rokhum, S.L. Green synthesis of silver nanoparticles using plant extracts and their antimicrobial activities: A review of recent literature. *RSC Adv.* **2021**, *11*, 2804-2837, <https://doi.org/10.1039/D0RA09941D>.
22. Hamid, H.A.; Mutazah, S.S.Z.R.; Yusoff, M.M. *Rhodomyrtus tomentosa*: A phytochemical and pharmacological review. *Asian J. Pharm. Clin. Res.* **2017**, *10*, 10-16, <https://doi.org/10.22159/ajpcr.2017.v10i1.12773>.
23. Nande, A.; Raut, S.; Michalska-Domanska, M.; Dhoble, S.J. Green Synthesis of Nanomaterials Using Plant Extract: A Review. *Curr. Pharm. Biotechnol.* **2021**, *22*, 1794-1811, <https://doi.org/10.2174/1389201021666201117121452>.
24. Mandal, S.; Marpu, S.B.; Hughes, R.; Omary, M.A.; Shi, S.Q. Green synthesis of silver nanoparticles using *Cannabis sativa* extracts and their antibacterial activity. *Green Sustain. Chem.* **2021**, *11*, 38-48, <https://doi.org/10.4236/gsc.2021.111004>.
25. Akintelu, S.A.; Olugbeko, S.C.; Folorunso, A.S. Green synthesis, characterization, and antifungal activity of synthesized silver nanoparticles (AgNPS) from *Garcinia kola* pulp extract. *BioNanoScience* **2021**, 1-11, <https://doi.org/10.1007/s12668-021-00925-3>.
26. Khoshnamvand, M.; Huo, C.; Liu, J. Silver nanoparticles synthesized using *Allium ampeloprasum* L. leaf extract: Characterization and performance in catalytic reduction of 4-nitrophenol and antioxidant activity. *J. Mol. Struct.* **2019**, *1175*, 90-96, <https://doi.org/10.1016/j.molstruc.2018.07.089>.
27. Kohsari, I.; Mohammad-Zadeh, M.; Minaeian, S.; Rezaee, M.; Barzegari, A.; Shariatinia, Z.; Koudehi, M. F.; Mirsadeghi, S.; Pourmortazavi, S. M. In vitro antibacterial property assessment of silver nanoparticles synthesized by *Falcaria vulgaris* aqueous extract against MDR bacteria. *J. Solgel. Sci. Technol.* **2019**, *90*, 380-389, <https://doi.org/10.1007/s10971-019-04961-0>.
28. Kong, H.S.; Musa, K.H.; Abdullah Sani, N. *Clinacanthus nutans* (Belalai Gajah/Sabah Snake Grass): antioxidant optimization on leaves and stems. In *AIP Conference Proceedings* **2016**, *1784*, 030030. AIP Publishing LLC, <https://doi.org/10.1063/1.4966768>.
29. Nahar, K.N.; Rahman, M.; Khan, G. M.; Islam, M.; Al-Reza, S.M. Green synthesis of silver nanoparticles from *Citrus sinensis* peel extract and its antibacterial potential. *Asian J. Green Chem.* **2021**, *5*, 135-150, <https://doi.org/10.22034/ajgc.2021.113966>.
30. Omran, B.A.; Nassar, H.N.; Fatthallah, N.A.; Hamdy, A.; El-Shatoury, E.H.; El-Gendy, N.S. Waste upcycling of *Citrus sinensis* peels as a green route for the synthesis of silver nanoparticles. *Energ. Source Part A* **2018**, *40*, 227-236, <https://doi.org/10.1080/15567036.2017.1410597>.
31. Ranoszek-Soliwoda, K.; Tomaszewska, E.; Małek, K.; Celichowski, G.; Orłowski, P.; Krzywowska, M.; Grobelny, J. The synthesis of monodisperse silver nanoparticles with plant extracts. *Colloids Surf. B* **2019**, *177*, 19-24, <https://doi.org/10.1016/j.colsurfb.2019.01.037>.



32. Sohal, J. K.; Saraf, A.; Shukla, K.K. Antimicrobial activity of biochemically synthesized silver nanoparticles (AgNPs) using Aloe vera gel extract. *J. Pharm. Innov.* **2019**, *8*, 376-382, <https://doi.org/10.14719/pst.2019.6.2.532>.